Solid-State Deuterium NMR and Molecular Modeling Studies of Conformational Dynamics in Carbohydrates

Baltzar Stevensson,[†] Christer Höög,[‡] Kai Ulfstedt-Jäkel,[†] Zhi Huang,[†] Göran Widmalm,[‡] and Arnold Maliniak*,[†]

Division of Physical Chemistry and Department of Organic Chemistry, Arrhenius Laboratory, Stockholm University, S-106 91 Stockholm, Sweden

Received: January 24, 2000; In Final Form: April 10, 2000

We report a deuterium nuclear magnetic resonance (NMR) investigation of octa-*O*-decanoylthio-β,β-trehalose (TTH-10) in the solid state. For the interpretation of deuterium NMR line shapes and spin−lattice relaxation rates, a two-site exchange model was invoked. The motional amplitude for the C−D vector in TTH-10 molecule was estimated to 72°, while the relative populations of the two sites were assumed to be temperature dependent. From the longitudinal deuterium relaxation rates, correlation times for the dynamic process were derived. We found these to be approximately 50 ns at 20 °C and 30 ns at 90 °C. In addition to NMR experiments, molecular dynamics (MD) computer simulations of octa-*O*-acetylthio-β,β-trehalose (TTH-2) and an oxygen analogue, octa-*O*-acetyl-β,β-trehalose (TH-2), were performed. The analysis of the two torsion angles relevant for the glycosidic linkage indicates that the conformations of the TTH-2 molecule essentially correspond to two states. This observation gives strong support for our assumption about the two-site exchange model used for interpretation of deuterium solid-state experiments.

Introduction

Investigations of molecular structure and dynamics in carbohydrates have recently attracted considerable attention. It is so because carbohydrates play a central role in biological systems in general and carbohydrate−receptor interactions in particular. Specialized carbohydrate binding proteins, known as lectins,[1] can distinguish configurational differences in sugar residues between, e.g., mannose and glucose. Various experimental and computational techniques have been employed in these studies.[2] In particular, several nuclear magnetic resonance (NMR) spectroscopy investigations devoted to molecular flexibility and dynamics in solution[3−5] and in the solid state[6−8] have been published. Recently, we reported studies of carbohydrates in different liquid crystalline phases. A tetrasaccharide, Lacto-*N*-neotetraose, was investigated by measurements of residual dipolar couplings in aqueous dilute liquid crystals.[9] Furthermore, using deuterium and carbon-13 NMR, we investigated a thermotropic, columnar mesophase formed by octa-*O*-decanoyl-β-cellobiose.[10,11]

We have continued to investigate carbohydrate systems and present herein a study of trehalose-related molecules. Compounds with different acyl groups were synthesized (Figure 1), and it turned out that these trehalose derivatives do not form liquid crystalline phases. Here we report an investigation of octa-*O*-decanoylthio-β,β-trehalose (TTH-10) in the solid state, using deuterium NMR. The TTH-10 compound was specifically deuterium labeled in the anomeric positions, **2d**.

Deuterium NMR is a powerful technique for studies of molecular order, structure, and dynamics in ordered systems. The advantage of the method is that the spectrum usually is simple and reflects only the behavior of a C−^{2}H bond. A disadvantage of the technique is the low natural abundance of deuterium, which requires specific isotopic labeling of the molecule.

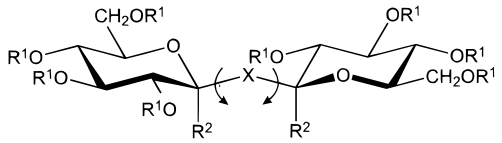

1 $R^1 = CH_3(CH_2)_6CO$, R^2 = H, X = S
2 $R^1 = CH_3(CH_2)_8CO$, R^2 = H, X = S
2d $R^1 = CH_3(CH_2)_8CO$, $R^2 = {}^2H$, X = S
3 $R^1 = CH_3(CH_2)_{10}CO$, R^2 = H, X = S
4 $R^1 = CH_3CO$, R^2 = H, X = S
5 $R^1 = CH_3CO$, R^2 = H, X = O

Figure 1. Schematic of β,β-trehalose derivatives investigated. The arrows indicate bond rotations related to the motion of the C−D vectors.

In contrast to isotropic liquids, where both intramolecular dynamics and tumbling motion are present, in the solid state the latter is completely absent. This enables studies of molecular conformations and internal dynamics.[12−14] In this work the deuterium line shapes, recorded in the solid state, were used for estimation of the geometry of molecular motion. The temperature dependence of the deuterium line shapes was employed for further characterization of the motional behavior of the C−^{2}H vector. The dynamic processes were also examined by measuring deuterium spin relaxation times. These were combined with parameters derived from the line shape analysis to provide correlation times which, in turn, define the time scale of the dynamic process.

In addition to the solid-state investigation we have performed molecular dynamics (MD) simulation of the octa-*O*-acetylthio-β,β-trehalose (TTH-2) and the corresponding oxygen analogue (TH-2). In the analysis of the MD trajectories we focused on defining conformational states and on identifying possible

* Author for correspondence: E-mail: arnold@physc.su.se.
† Division of Physical Chemistry.
‡ Department of Organic Chemistry.

10.1021/jp0002805 CCC: $19.00
Published on Web 06/03/2000

transitions between these states. We have also investigated the effect of sulfur/oxygen substitution in the glycosidic linkage on the molecular conformations.

Experimental and Computational Details

Synthesis. The β,β-thiotrehalose core was prepared according to the procedure of Schneider and Wrede.[15] Reduction of the D-gluconic acid lactone (6.0 g, 33.7 mmol) to [1-^{2}H]-D-glucose with $NaBD_4$ (540 mg, 12.9 mmol) was performed in ^2H_2O (30 mL) at ambient temperature for 2 h. The solution was neutralized with Dowex-50(H^+), evaporated to dryness, and coevaporated three times with methanol (30 mL). [1-^{2}H]-D-Glucose was then transformed into 2,3,4,6-tetra-*O*-acetyl-[1-^{2}H]-α-D-glucopyranosyl bromide according to Lemieux.[16] Acylation was performed by slow addition of the acyl chloride (25 mmol) to a solution of β,β-thiotrehalose (500 mg, 1.4 mmol) in THF (10 mL) and pyridine (10 mL). The mixture was then refluxed for 3 h. Toluene (50 mL) was added and the mixture extracted with water (10 mL), two times with aqueous HCl (1 M, 25 mL) and two times with saturated aqueous $NaHCO_3$ (25 mL). The organic phase was dried over $MgSO_4$, filtered, and concentrated under reduced pressure. Recrystallization was performed several times from THF/MeOH. Typical yields were ∼40%. The acyl chlorides used were octanoyl chloride, decanoyl chloride, and dodecanoyl chloride for **1**, **2**, and **3**, respectively.

Characterization. The molecular mass was determined by fast atom bombardment mass spectrometry (FABMS) on a JEOL SX-102 instrument in the positive mode using glycerol/thioglycerol as a matrix and a resolution of 2500. The *m*/*z* values observed were 1366 for **1**, 1590 for **2**, 1592 for **2d**, and 1814 for **3**. Melting points were observed at 95−98 °C for **1**, 93−96 °C for **2**, and 89−94 °C for **3**. Only one transition at 89 °C was observed for **2** in differential scanning calorimetry using a Perkin-Elmer DSC-2C instrument. Selected NMR data are given below. ^{13}C NMR of **1**: 14.0 (Me), 22.6−34.0 (CH_2), 62.0 (C6), 68.2, 70.0, 73.6, 76.4 (C2−C5), 80.7 (C1), 172.0 (2C), 172.7, 173.3. ^{1}H NMR of **1**: 4.83 (H1, d, 9.9 Hz). For **2** and **3** the NMR data were essentially identical with some additional signals at ∼29 ppm in the ^{13}C NMR spectrum. In **2d** the anomeric proton was absent and the signal from C1 was a triplet. Proton and carbon-13 NMR spectra were recorded in $CDCl_3$ at 30 °C on a JEOL spectrometer (6.3 T) and referenced to internal TMS at 0.0 ppm.

Deuterium NMR Experiments. All solid state ^{2}H NMR measurements were performed on a Chemagnetics CMX400 spectrometer operating at a magnetic field strength of 9.4 T, corresponding to the deuterium frequency of 61.4 MHz. A high-power probe was used with a 5 mm horizontal solenoid coil. The ^{2}H NMR spectra were recorded using a standard solid-echo sequence, $90_x°-t_1-90_{\pm y}°-t_2-acq$, with a 90° pulse length of typically 2.5−3.0 μs and a recycle delay of at least 5 times the spin−lattice relaxation time. The echo delay, t_1, was set to 20 μs and t_2 was carefully chosen so that the first point of the free induction decay (FID) was digitized at the echo maximum. For a typical spectrum in the solid phase 10 000 transients were accumulated. The ^{2}H spin−lattice relaxation rates, T_1^{-1}, were measured by the conventional inversion recovery technique using a quadrupole echo for signal detection. Reported nuclear spin relaxation times are averages of at least three measurements. In the liquid phase the deuterium spectra were obtained using a single pulse experiment while spin−lattice relaxation times were determined using the standard inversion recovery pulse sequence. Based on reproducibility, the random error in this experimental data set is estimated to be on the order of 10%.

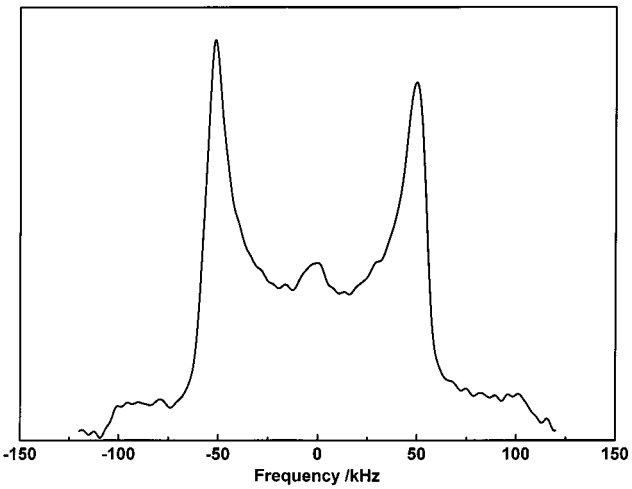

Figure 2. Deuterium NMR spectrum of **2d** (TTH-10) recorded at 30 °C.

Computer Simulations. The molecular dynamics simulations of isolated molecules were performed using the Discover program within the Insight II package and the CVFF[17] force field. In order to limit the number of interacting sites, the simulations were performed on octa-*O*-acetylthio-β,β-trehalose (TTH-2) and a corresponding oxygen analogue, octa-*O*-acetyl-β,β-trehalose (TH-2). The simulations were carried out at 300 K and the temperature was kept constant (NVT ensemble) using the Nosé algorithm.[18] The equations of motion were integrated using a time step of 1 fs, and the trajectory files were saved every 100 steps. The simulations covered 100 ps of equilibration followed by production runs of 5 ns for each molecule.

Results and Discussion

Deuterium NMR Line Shape Analysis. Deuterium NMR spectra for the TTH-10 compound were recorded in the temperature range between 20 and 125 °C. A single phase transition corresponding to melting of the solid phase was observed at 90 °C. This is in good agreement with differential scanning calorimetry where the transition was observed at 89 °C. A solid−liquid transition in deuterium NMR is easily identified since it results in a dramatic narrowing of the line shape due to onset of the molecular tumbling, absent in the solid state. In Figure 2 we show a deuterium line shape of TTH-10 in the solid state recorded at 30 °C. The spectrum is essentially uniaxial with a quadrupolar splitting of 100 kHz. In fact, uniaxial spectra were observed in the entire investigated temperature interval of the solid phase, i.e., 20−90 °C.

The deuteron is a spin $I = 1$ nucleus which, in addition to a magnetic dipole, possesses an electric quadrupole. The latter interacts with the electric field gradient (EFG) and gives rise to a shift in frequency which in turn depends on a relative orientation of the static magnetic field, B_0, and the EFG tensor. The sensitivity of the deuterium spectrum to motional rates can be determined by monitoring the T_2 anisotropy.[19] No significant line shape distortions in the entire temperature range were observed when the t_1 delay in the quadrupole echo was varied. Thus, we conclude that the motion is rapid compared to the quadrupolar interaction. We will return to this issue in the next section. In the fast motion limit ($\nu_{motion} > 10^7$ s^{-1}) the observed deuterium frequency is a population weighted average of each orientation. The spectrum is defined by the principal components $|\bar{\nu}_z| > |\bar{\nu}_y| \geq |\bar{\nu}_x|$, which can be expressed in terms of the

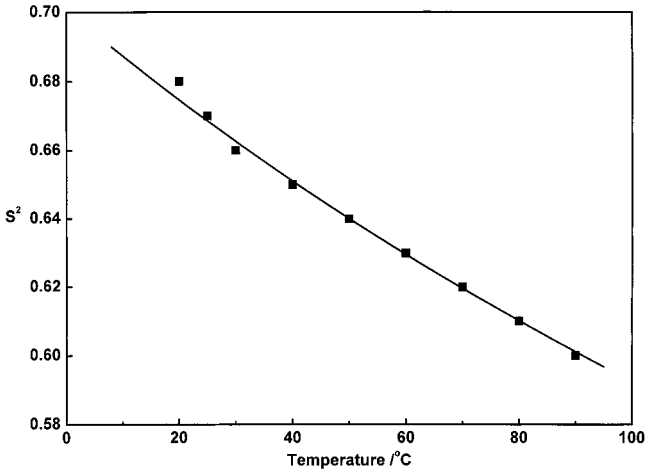

Figure 3. The generalized order parameter, S^2, for TTH-10 derived from eq 1. The continuous line was calculated using eq 4 with the following parameters: $\nu_q = 123$ kHz, $\Theta = 72°$, $\Delta E = 3.7$ kJ mol^{-1}, $A = 0.7$.

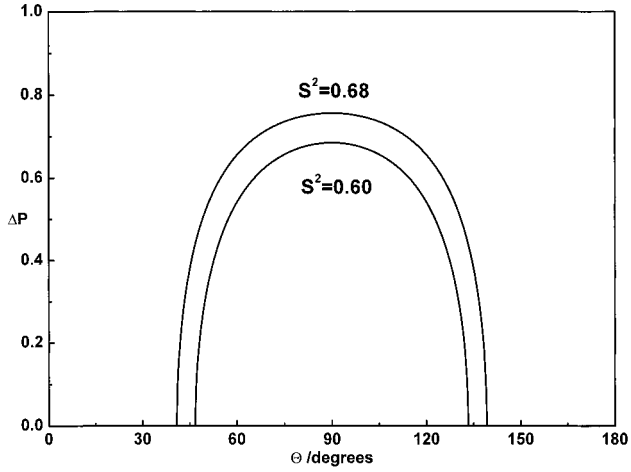

Figure 4. Population differences, $\Delta P = P_2 - P_1$, versus jump angle, Θ, corresponding to highest and lowest values of the generalized order parameter.

generalized order parameter, S^2 [20−22]

$$S^2 = \frac{2}{3}\frac{\bar{\nu}_x^{\,2} + \bar{\nu}_y^{\,2} + \bar{\nu}_z^{\,2}}{\nu_q^{\,2}} = \left[\frac{\bar{\nu}_q}{\nu_q}\right]^2 \qquad (1)$$

where the last equality applies to a uniaxial spectrum, $4\nu_q/3$ is the quadrupole coupling constant, e^2qQ/h, and $\bar{\nu}_q$ is the quadrupolar splitting. The static EFG tensor is assumed to be axially symmetric, with the unique tensor axis parallel to the C−^{2}H bond. A typical value of a quadrupole coupling constant for such a bond is 165 kHz,[23,24] and we adopt this value in the following analysis. The temperature dependence of S^2 is shown in Figure 3. Note that a completely rigid C−D vector is characterized by $S^2 = 1$ and low values of S^2 indicate no spatial restrictions, and thus large flexibility. The generalized order parameter in Figure 3 is in the range 0.6−0.7, which is lower than measured for other, oxygen-based, disaccharides in the liquid phase.[25]

In order to interpret the deuterium line shape in terms of molecular motional parameters, a dynamical model is required.[26] We anticipate the simple case of a rapid exchange of the C−D bond between two orientations. The relation between the generalized order parameter, S^2, and the motional parameters is given by[22,27]

$$S^2 = 1 - 3P_1P_2\sin^2\Theta \qquad (2)$$

where Θ is the jump angle and P_1 and P_2 are the relative populations ($P_1 + P_2 = 1$) of each site. The motional process that determines the jumps of the C−D vector is indicated by the arrows in Figure 1. First, we examine the range of angles Θ and populations that are consistent with the experimentally determined S^2 values. In Figure 4 plots of $\Delta P = P_2 - P_1$ versus Θ are displayed for the two limiting values (at highest and lowest temperatures) of the order parameter. We note that a wide range of Θ and ΔP values is allowed. Therefore, further assumptions are needed for a quantitative analysis of the motional parameters. For a two-site jump model there are, in principle, three possibilities to describe the temperature dependence of the deuterium NMR spectra: (a) the jump angle varies, (b) the population ratio, P_1/P_2, changes, and (c) both the amplitude and the populations vary with temperature. Most probably the real situation corresponds to case c, but in order to make the problem more tractable we assume that the jump angle is constant, case b, in the solid phase and that the temperature dependence of S^2 is dictated by the Boltzmann distribution:[28]

$$\frac{P_1}{P_2} = \frac{P_1}{1 - P_1} = A\exp\left(-\frac{\Delta E}{RT}\right) \qquad (3)$$

which inserted in eq 2 gives

$$S^2 = 1 - 3\frac{A\exp(-\Delta E/RT)}{[1 + A\exp(-\Delta E/RT)]^2}\sin^2\Theta \qquad (4)$$

where $\Delta E = E_1 - E_2$ is the energy difference between the two sites and A is related to the entropy difference: $\Delta S = S_1 - S_2 = R\ln A$. Equation 4 was numerically fitted to the experimentally determined values of S^2 using a nonlinear least squares search program based on the subroutine STEPIT.[29] The fitting procedure consisted of two steps: first a random (Monte Carlo) scan for initial parameters, followed by a minimization of the error squares sum:

$$\text{error} = \sum_i [S_i^2(\text{exp}) - S_i^2(\text{calc})]^2 \qquad (5)$$

The values of the three parameters, Θ, ΔE, and A, derived in the fitting procedure were 72° ± 5, 3.7 ± 0.1 kJ mol^{-1}, and 0.7 ± 0.1, respectively. These parameters were used to calculate the continuous curve in Figure 3. Note that the jump angle of 72° corresponds to a bond rotation, indicated in Figure 1, of 77°. In order to further investigate the validity of the assumption about constant motional amplitude, we consider the cone model. Here, the C−^{2}H vector diffuses freely in a cone of semiangle Θ_c which is related to the generalized order parameter, S^2, by[30]

$$S = \left[\cos\Theta_c\frac{1 + \cos\Theta_c}{2}\right] \qquad (6)$$

Using experimentally obtained S^2 values (Figure 3), the cone semiangles are restricted to values between 29° and 34° for the lowest and highest temperatures, respectively. These semiangles correspond the motional amplitude of 58−68° which is in reasonable agreement with the jump angle, $\Theta = 72°$, derived from the two-site exchange model.

Nuclear Spin Relaxation and Conformational Dynamics. In order to determine the rates for the motional process, the

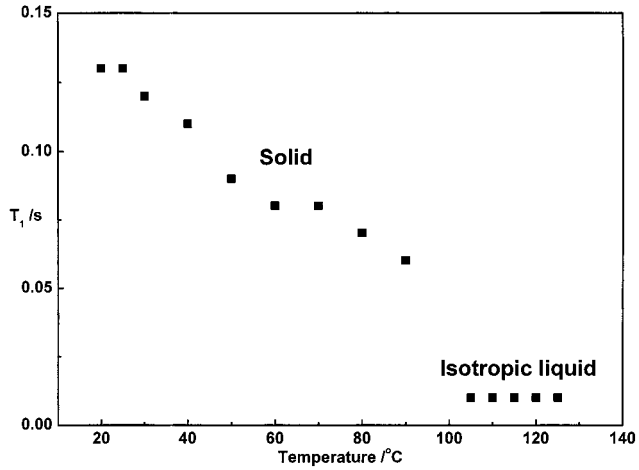

Figure 5. Temperature dependence of the deuterium spin−lattice relaxation times in TTH-10.

deuterium longitudinal relaxation time constant, T_1, was measured. The temperature dependence of T_1 is shown in Figure 5. We note that at 90 °C a drastic shortening of T_1 occurs which corresponds to the solid−liquid phase transition. In analogy with the narrowing of the spectra, the reduction of T_1 is due to the onset of the molecular tumbling in the isotropic phase. We limit our analysis to the solid state, where we believe that the spin relaxation reflects solely the internal dynamics of the C−^{2}H vector.

The expression for the deuterium spin−lattice relaxation time in the case of the two-site jump model is given by[31]

$$\frac{1}{T_1} = \frac{(2\pi\nu_q)^2}{2} P_1 P_2 \sin^2\Theta\left[g(\tau,\omega)\left(B_4 - \left(\frac{3}{4}B_1 - B_2\right)\cos 2\varphi\right) + g(\tau,2\omega)(4B_5 - 4B_2\cos 2\varphi)\right] \quad (7)$$

where the spectral density function is assumed to be

$$g(\tau,\omega) = \frac{\tau}{1 + (\omega\tau)^2} \quad (8)$$

where ω is the Larmor frequency, the angular coefficients $B_i(\theta)$ are tabulated in ref 31, and the polar angles θ, φ define the orientation of the magnetic field, $\mathbf{B}_0$, in the motionally averaged quadrupole tensor principal axis system. The correlation time, τ, is defined using the jump rates between the sites, $\tau = [k_{12} + k_{21}]^{-1}$. In general, the relaxation rates in solids are orientation dependent (θ, φ dependence in eq 7). The reported T_1 values were determined for the spectral cusps, i.e., $\theta = 90°$ and $\varphi = 0°$. We did not observe any frequency anisotropy in the whole temperature range of the solid phase. This result indicates that the deuterium longitudinal relaxation rates in the TTH-10 molecule are indeed orientation independent. In Figure 6 we show temperature dependence of the correlation times derived from the spin−lattice relaxation rates using eq 7. At the lowest temperature (20 °C) the correlation time is 55 ns while the corresponding value at 90 °C, i.e., close to the phase transition to the isotropic phase, is 32 ns. The rates for the exchange process confirm indeed the fast limit assumption used in the line shape analysis. The plot is essentially linear which justifies an assumption about a simple Arrhenius relation. The apparent activation energy of 6.5 kJ mol^{-1} was determined.

Molecular Dynamics Simulations. The normalized distribution functions for the torsion angles ϕ and ϕ' in **4** (TTH-2) and in the oxygen analogue **5** (TH-2) were generated in MD simulations using the CVFF force field. These functions are shown in Figure 7. Dictated by the molecular symmetry, distributions corresponding to the two Ramachandran angles, ϕ and ϕ', should be identical. They are nearly so, except for the noise observed in particular in the TTH-2 distributions. The angles are defined as H−C−X−C, with X = S or O. These torsion angles are related to the glycosidic linkage and determine the intramolecular motion of the C−D bonds, monitored by deuterium NMR. The difference between the distributions in the two molecules is very clear: while TH-2 shows a single maximum at 60°, two maxima at 60° and 160° are observed for the TTH-2 molecule. The shape of the distribution function gives support to our two−site jump model used for the interpretation of the deuterium NMR data of TTH-10 in the solid state. In fact, the amplitude of the torsional motion derived from the experiments (77°) is also in reasonable agreement with simulation results. The ratio between the relative populations, P_1/P_2, differs however significantly: the experimental results predict a ratio $P_1/P_2 \approx 0.2$, whereas the computer simulation indicates equally populated sites. This deviation may origin from different molecular environments in the experiments and in computer simulations.

The distribution functions shown in Figure 7 are consistent with previously reported results,[32] where NMR spectroscopy in solution and molecular mechanics computations predict *O*-linked disaccharide to be essentially monoconformational, while the thio analogue shows two conformational states populated to a large extent.

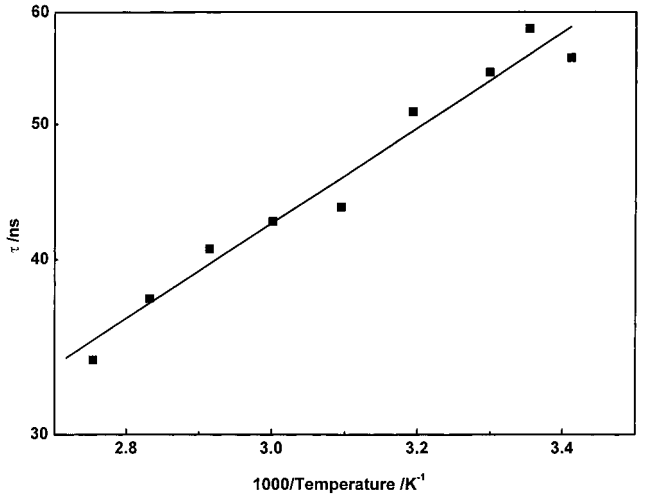

Figure 6. Temperature dependence of the correlation time for the two-site jump process in TTH-10.

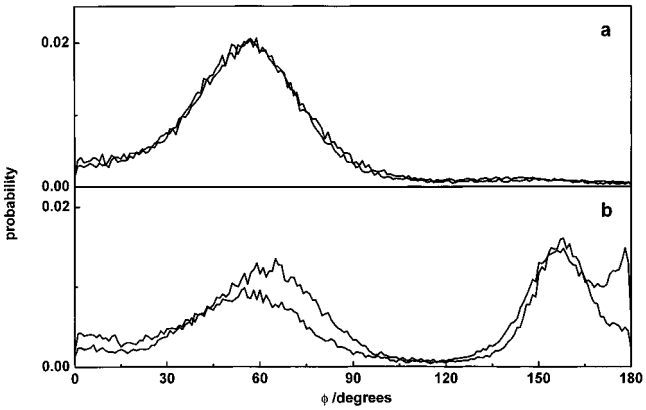

Figure 7. Distribution functions of the torsion angles ϕ and ϕ' for (a) TH-2 and (b) TTH-2 molecules determined from MD trajectories.

Recently, quantum chemical (ab initio) calculations of several 2-substituted tetrahydropyran compounds were reported.[33] In that study oxygen ($-OCH_3$) and sulfur ($-SCH_3$) substituted molecules were included. The calculations predict the most stable conformation for both oxygen and sulfur compounds to be that with the torsional angle $\phi = 60°$. The state where $\phi = 180°$ is a local energy minimum. For the oxygen compound the energy difference between these states is 14.3 kJ mol^{-1}, while for the sulfur analogue it corresponds to 5.5 kJ mol^{-1}. The transition states for oxygen and sulfur molecules are at ~40 and ~25 kJ mol^{-1}, respectively. These results are in fact in good agreement with our MD analysis. Two states of the sulfur compound are populated, while only the lowest state of the oxygen molecule is observed. The major difference between the ab initio calculations and MD results is that a reversed order of stability is observed for the sulfur compound. However, in view of nearly equal distribution intensities in Figure 7 and a relative small energy difference between the states (5.5 kJ mol^{-1}), this discrepancy seems not to be very serious. The different conformational behavior of the two molecules can be explained by different bond distances. The C−O bond length, determined in the ab initio calculations, is 1.40 Å while the corresponding value for a C−S bond is 1.81 Å. However, the C−X−C angle which is 115° in the oxygen molecule is reduced to 100° when X = S. Thus, the electrostatic repulsion between lone-pair orbitals on the central atom in the glycosidic bond and the oxygen atoms in the ring are much stronger in the oxygen molecule (X = O). We conclude, therefore, that the *exo-anomeric effect* is more pronounced in TH-2 than in TTH-2.

Deuterium line shapes in the fast motion region provide information about the generalized order parameter (S^2). This parameter measures the degree of spatial restriction related to the local motion of a vector (C−D bond in the experiments, and C−H bond in the simulation) in the molecule. From an MD trajectory the generalized order parameter, S^2, is conveniently determined as the equilibrium time average:[21,34]

$$S^2 = {}^3/_2[\langle x^2\rangle^2 + \langle y^2\rangle + \langle z^2\rangle^2 + 2\langle xy\rangle^2 + 2\langle xz\rangle^2 + 2\langle yz\rangle^2] - {}^1/_2 \quad (9)$$

where x, y, and z are projections of the C−H vector on the x, y, and z axes related to the moment of inertia tensor in the molecule. S^2 determined for the two anomeric C−H vectors in TTH-2 molecule were 0.31 and 0.36; the corresponding values for the oxygen analogue, TH-2, were 0.32 and 0.32. In view of very different torsion distribution functions (Figure 7), the similar order parameters may look surprising. A possible explanation is, however, that the large amplitude jumps in the sulfur compound are nearly compensated by significant librations occurring in the potential well of the oxygen molecule. Note that the latter distribution functions (Figure 7a) are very broad. The values of S^2 calculated from the trajectory are lower than those determined from the experiments. This fact is not surprising since the simulations were carried out on isolated molecules while the experiments were performed in the solid state.

Summary

The objective of this paper has been to study conformational dynamics of octa-*O*-decanoylthio-β,β-trehalose (TTH-10) in the solid state. To that end, a specifically deuterium labeled compound was prepared and the investigation was performed by means of solid-state NMR spectroscopy. In addition, molecular dynamics (MD) computer simulations of octa-*O*-acetylthio-β,β-trehalose (TTH-2) and an oxygen analogue octa-*O*-acetyl-β,β-trehalose (TH-2) were performed.

For the interpretation of deuterium NMR line shapes and spin−lattice relaxation rates, a two-site exchange model was invoked. Assuming that the temperature dependence of NMR spectra is solely due to a change of populations of the sites, the jump angle and the energy difference between the two states were estimated. The jump angle of 72° for the C−D vector in the TTH-10 molecule was obtained from the analysis, which corresponds to the bond rotation of 77°. The energy difference between the states was of the order of 4 kJ mol^{-1}. We also considered a motional model in which the C−D bond is wobbling within a cone of semiangle Θ_c. The average value of this semiangle was estimated to 32°, corresponding to a maximum motional amplitude of 64°. These large amplitude jumps in the solid state may appear surprising. In view of the waxlike properties of TTH-10, it can probably be classified as disordered or a highly "fluid" solid. It would therefore be interesting to determine thermodynamic parameters for the melting of TTH-10. From the longitudinal deuterium relaxation rates, correlation times for the dynamic process were derived. We found these to be approximately 50 ns at 20 °C and 30 ns at 90 °C.

The purpose of the computer simulations was to investigate the dynamical processes in the carbohydrate part of the molecules, and therefore the decanoyl chains were replaced by acetyl groups. The analysis of the two torsion angles relevant for the glycosidic linkage indicates that the conformations of the TTH-2 molecule essentially correspond to two states. This observation gives strong support for our assumption about the two-site exchange model used for the interpretation of deuterium solid-state experiments. The oxygen analogue, TH-2, shows a completely different conformational behavior. The molecule shows only a single state with high amplitude librations. The interpretation of the experimental results and the analysis of the trajectories are in good agreement with ab initio quantum chemical calculations on similar compounds. An interesting complement to the present study would be an investigation of deuterium-labeled oxygen analogue octa-*O*-decanoyl-β,β-trehalose (TH-10). The synthesis of this compound is now in progress.

We conclude this article by pointing out the power of combination of solid-state NMR spectroscopy and molecular modeling techniques. In particular, the conformational analysis of an MD trajectory provides an important insight into intramolecular dynamics.

Acknowledgment. We thank Dick Sandström for valuable comments on the manuscript. This work was supported by grants from the Swedish Natural Science Research Council and Carl Trygger Foundation. Z.H. thanks the Wenner-Gren Center Foundation for financial support.

References and Notes

(1) Lis, H.; Sharon, N. *Chem. Rev.* **1998**, *98*, 637.

(2) Widmalm, G. In *Carbohydrate Chemistry;* Boons, G.-J., Ed.; Kluwer Academic Publishers: Dordrecht, 1997; pp 448−502.

(3) Kjellberg, A.; Rundlöf, T.; Kowalewski, J.; Widmalm, G. *J. Phys. Chem. B* **1998**, *102*, 1013.

(4) Mäler, L.; Lang, J.; Widmalm, G.; Kowalewski, J. *Magn. Reson. Chem.* **1995**, *33*, 541.

(5) Batta, G.; Köver, K. E.; Gervay, J.; Hornyák, M.; Roberts, G. M. *J. Am. Chem. Soc.* **1997**, *119*, 1336.

(6) Zhang, P.; Klymachyov, A. N.; Brown, S.; Ellington, J. G.; Grandinetti, P. J. *Solid State Nucl. Magn. Reson.* **1998**, *12*, 221.

(7) Hatcher, M. E.; Mattiello, D. L.; Meints, G. A.; Orban, J.; Drobny, G. P. *J. Am. Chem. Soc.* **1998**, *120*, 9850.
(8) Ravindranathan, S.; Feng, X.; Karlsson, T.; Widmalm, G.; Levitt, M. H. *J. Am. Chem. Soc.* **2000**, *122*, 1102.
(9) Rundlöf, T.; Landersjö, C.; Lycknert, K.; Maliniak, A.; Widmalm, G. *Magn. Reson. Chem.* **1998**, *36*, 773.
(10) Sandström, D.; Stenutz, R.; Widmalm, G.; Maliniak, A. *J. Chem. Soc., Faraday Trans.* **1996**, *92*, 111.
(11) Huang, Z.; Sandström, D.; Henriksson, U.; Maliniak, A. *J. Phys. Chem. B* **1998**, *102*, 8395.
(12) Zaborowski, E.; Zimmermann, H.; Vega, S. *J. Am. Chem. Soc.* **1998**, *120*, 8113.
(13) Wiliams, J. C.; McDermott, A. E. *J. Phys. Chem. B* **1998**, *102*, 6248.
(14) Kamihira, M.; Naito, A.; Tuzi, S.; Saitô, H. *J. Phys. Chem. A* **1999**, *103*, 3356.
(15) Schneider, W.; Wrede, F. *Ber. Dtsch. Chem. Ges.* **1917**, *50*, 793.
(16) Lemieux, R. U. *Meth. Carbohydr. Chem.* **1963**, *2*, 221.
(17) Dauber-Osguthorpe, P.; Roberts, V. A.; Osguthorpe, D. J.; Wolff, J.; Genest, M.; Hagler, A. T. *Proteins: Struct., Funct., Genet*. **1988**, *4*, 31.
(18) Nosé, S. *J. Chem. Phys.* **1984**, *81*, 511.
(19) Vega, A. J.; Luz, Z. *J. Chem. Phys.* **1987**, *86*, 1803.
(20) Torchia, D. A.; Szabo, A. *J. Magn. Reson*. **1985**, *64*, 135.
(21) Henry, E. R.; Szabo, A. *J. Chem. Phys.* **1985**, *82*, 4753.
(22) Sparks, S. W.; Budhu, N.; Young, P. E.; Torchia, D. A. *J. Am. Chem. Soc*. **1988**, *110*, 3359.
(23) Spiess, H. W. *Adv. Polym. Sci*. **1985**, *66*, 23.
(24) Aliev, A. E.; Harris, K. D. M.; Mahdyarfar, A. *J. Chem. Soc., Faraday Trans.* **1995**, *91*, 2017.
(25) Söderman, P.; Widmalm, G. *Magn. Reson. Chem*. **1999**, *37*, 586.
(26) Wittebort, R. J.; Olejniczak, E. T.; Griffin, R. G. *J. Chem. Phys*. **1987**, *86*, 5411.
(27) Hirschinger, J.; English, A. D. *J. Magn. Reson*. **1989**, *85*, 542.
(28) Maliniak, A.; Greenbaum, S.; Poupko, R.; Zimmermann, H.; Luz, Z. *J. Phys. Chem*. **1993**, *97*, 4832.
(29) Chandler, J. P. *STEPIT* (Program No. 307); QCPE; Chemistry Department, Indiana University, Bloomington, IN, 1982.
(30) Lipari, G.; Szabo, A. *Biophys. J*. **1980**, *30*, 489.
(31) Torchia, D. A.; Szabo, A. *J. Magn. Reson*. **1982**, *49*, 107.
(32) Aguilera, B.; Jimenéz-Barbero, J.; Fernánez-Mayoralas, A. *Carbohydr. Res.* **1998**, *308*, 19.
(33) Tvaroška, I.; Carver, J. P. *J. Phys. Chem*. **1996**, *100*, 11305.
(34) Pastor, R. W.;Venable, R. M. In *Computer Simulation of Biomolecular Systems*; van Gunsteren, W. F., Weiner, P. K., Wilkinson, A. J., Eds.; ESCOM: Leiden, 1993; pp 443−463.